Observation of the Helical Structure of the Bacterial Polysaccharide Acetan by Atomic Force Microscopy

Andrew R. Kirby, A. Patrick Gunning, Victor J. Morris, and Michael J. Ridout
Institute of Food Research, Norwich Research Park, Colney, Norwich NR4 7UA, United Kingdom

ABSTRACT A method has been developed that has been found to give reproducible images of uncoated polysaccharides by Atomic Force Microscopy (AFM). Aqueous solutions of the polysaccharide are deposited as drops onto freshly cleaved mica surfaces, air dried, and then imaged under butanol. The method has been used to obtain images of the bacterial polysaccharide acetan. In regions within the deposited sample, where the molecules are aligned side-by-side, it has been possible to observe a periodic structure along the polysaccharide chain, attributable to the helical structure of acetan.

INTRODUCTION

Polysaccharides are interesting candidates for study by scanning probe microscopy. Most polysaccharides are complex irregular, possibly branched, structures that are difficult to characterize by conventional biophysical methods. For polysaccharides with regular chemical repeats, the helical structures can be analyzed, at atomic resolution, by means of x-ray diffraction of oriented fibers (Arnott, 1977). If oligosaccharides can be coaxed into forming single crystals, then electron diffraction and microscopy provide a powerful combination of methods for evaluating molecular structure (Perez and Chanzy, 1989; Perez and Revol, 1993). However, most electron microscopy studies on individual polysaccharides have been made on metal-coated samples or replicas for which the resolution is limited by the grain size of the metal coating (Stokke et al., 1987). Scanning probe microscopy offers the prospect of achieving higher resolution, under ambient conditions, in gaseous or fluid environments. At present there are very few scanning probe microscopy studies on polysaccharides (Rabe et al., 1990; Yang et al., 1990; Miles et al., 1991; Shigekawa et al., 1991, Hanley et al., 1992; Lee et al., 1992; Meyer et al., 1992; Oka and Takahashi, 1992; Gunning et al., 1993; Wilkins et al., 1993). Most of these studies have been made by scanning tunnelling microscopy (STM) (Rabe et al., 1990; Yang et al., 1990; Miles et al., 1991; Shigekawa et al., 1991; Lee et al., 1992; Oka and Takahashi, 1992; Gunning et al., 1993; Wilkins et al., 1993) and have tended to emphasize the difficulties involved in the imaging of these materials. In many cases only single images of individual "molecules" have been presented, and the results have not been reproduced by other researchers, even in studies on the same polysaccharide (Miles et al., 1991; Gunning et al., 1993; Wilkins et al., 1993). Wilkins and coworkers (Wilkins et al., 1993) have reported comparative STM and electron microscopy studies on xanthan. These authors resorted to the use of spray deposition followed by metal coating. Such treatment has led to the most reproducible STM pictures of xanthan obtained at the present time. However, this method is limited in resolution by the grain size of the metal coating. To investigate the molecular architecture of polysaccharides, it is necessary to develop reproducible methods for imaging uncoated polysaccharides by scanning probe microscopy, thus preserving the inherent higher resolution of these techniques. AFM offers advantages over the use of STM such as the ability to control imaging forces, wider choice of more suitable substrates, and much easier interpretation of images to name but a few. At present there are only two reports of AFM studies on polysaccharides (Hanley et al., 1992; Meyer et al., 1992). Hanley and co-workers report studies on cellulose microfibrils using both electron microscopy and AFM (Hanley et al., 1992). The authors claim to observe periodicities associated with the cellulose helix at the surface of the crystalline structures. Meyer and co-workers (Meyer et al., 1992) report a preliminary account of AFM studies of xanthan monolayers adsorbed onto mica. However, the images presented are of continuous periodic arrays with no visible polymer ends or defects.

In this article, we report studies on the bacterial polysaccharide acetan using a method that we have found to be reliable for imaging a range of polysaccharides.

MATERIALS AND METHODS

Acetan is the anionic heteropolysaccharide secreted by the bacterium *Acetobacter xylinum* NRRL B42 (NC1B 40123) (Couso et al., 1987). Growth conditions for the production of acetan using the wild-type parent strain of *A. xylinum*, and cellulose-minus mutants, have been described in detail elsewhere (MacCormick et al., 1993). Acetan was isolated from the culture broths using the following procedure: the culture broth was centrifuged (23×10^3 *g*, 30 min) to remove bacterial cells, and KCl was added to a final concentration of 1% w/v. The total polysaccharide content of the broth was collected by alcohol precipitation, and the anionic polysaccharide acetan was isolated by a subsequent selective precipitation with cetyl trimethyl ammonium bromide (CTAB) using the methodology described by Scott (1965). The final freeze-dried product is in the sodium salt form. The purity of the sample was checked by neutral sugar and methylation analysis as described elsewhere (MacCormick et al., 1993).

The powdered acetan was dispersed in deionized distilled water (1 mg ml^{-1}), heated to 85°C in a sealed tube for 1 h, and then cooled to room

Received for publication 24 August 1994 and in final form 3 October 1994.
Address reprint requests to Dr. Victor J. Morris, Institute of Food Research, Norwich Research Park, Colney, Norwich NR4 7UA, U.K. Tel.: 01-603-255000; Fax: 01-603-507723.

0006-3495/95/01/360/04 $2.00

temperature. The sample was diluted (0.1 mg ml^{-1}), reheated at 85°C in a sealed tube for 1 h, and then cooled to room temperature. Finally, the sample was diluted to 0.01 mg ml^{-1}, reheated at 85°C for 1 h in a sealed tube, and then cooled to room temperature. This rather elaborate preparation was done initially to determine accurately the most suitable concentration to give appropriate coverage of molecules on the mica. Subsequent experiments have shown that a one-step dilution from 1 mg ml^{-1} to 0.01 mg ml^{-1} works just as well as long as the heating steps are not omitted. Heating is required to ensure that the sample is fully dissolved and to minimize the presence of very large aggregates. A 2 μl drop was deposited onto freshly cleaved mica and allowed to dry in air for 10 min. The sample was then imaged under butanol (Sigma Chemical Co., St. Louis, MO). Butanol was chosen for several reasons. First, it is difficult to image biopolymers deposited on to mica in air using standard AFM tips under ambient conditions (i.e., relative humidity > 30%). This is due to the presence of a thin layer of water on top of the sample (and/or tip). As the tip is advanced toward the sample, a strong capillary force rams the tip down onto the sample exerting forces many times greater than can be tolerated by fragile macromolecules without suffering damage (Drake et al., 1989; Weisenhorn et al., 1989; Bustamante et al., 1992; Thundat et al., 1992a, b; Vesenka et al., 1992). This effect can be eliminated by imaging under water, thereby removing the meniscus that would otherwise form at the tip-sample interface. Unfortunately, even with the water-mica interface there is another effect, still not completely understood, that manifests itself as a large adhesive force between the AFM tip and the mica surface (Hansma et al., 1993). However this effect can be minimized by imaging under alcohols rather than water. This empirical observation has led to the reliable imaging of nucleic acids deposited onto mica (Hansma et al., 1992a, b; Li et al., 1992; Hansma and Hansma, 1993; Murray et al., 1993). Second, alcohols such as butanol are precipitants for polysaccharides and therefore might be expected to inhibit desorption of the polysaccharide from the mica surface.

The atomic force microscope used in the present studies was an ECS (East Coast Scientific, Cambridge, UK) instrument. The sample was contained in a liquid cell and imaged using constant force conditions. Optimum imaging conditions used forces ~3–4 nN. The tips used were the short narrow variety of nanoprobe cantilevers (Digital Instruments, Santa Barbara, CA) with a nominal force constant of 0.38 Nm^{-1}.

RESULTS

A typical network of uncoated acetan molecules is shown in Fig. 1. The density of polymer chains observed is dependent upon the initial polymer concentration but varies considerably within a deposit on the mica. The contrast observed in the image is dependent upon the applied force. For forces <1 nN, the contrast is poor and it is difficult to identify polymer chains. At larger values >10 nN, the force is sufficient to distort and damage the polysaccharides. Forces in the range 3–4 nN give optimum contrast without causing damage to the molecules. Within the image (Fig. 1), it is possible to identify individual molecules and the ends of molecules. There does not appear to be any preferential alignment or orientation of the strands suggesting that the drying process has not influenced the apparent shape of the molecules. There is also evidence (e.g., Fig. 1 *A*) for inter-molecular entwining of the polymer chains. Measurements of the thickness of individual strands indicates values of the order of 10 nm. These high values are much larger than would be expected for individual polymer chains and are probably the result of the finite size of the AFM tip with respect to the molecular thickness. As the tip scans across the molecule, different regions of the tip interact with the molecule causing a broadening of the image. This effect has been reported for the imaging of DNA samples, and the broadening effect can be reduced by the use of sharper "supertips" (Hansma et al., 1992b). Evidence to be presented later in this article also supports this assertion.

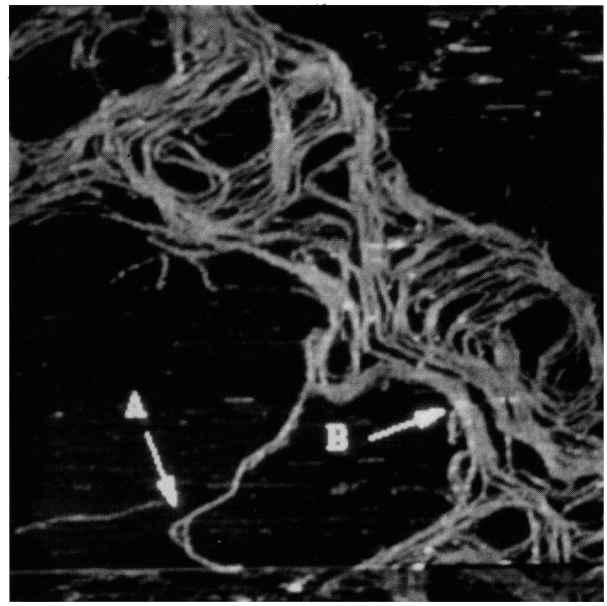

FIGURE 1 AFM images of acetan deposited onto mica and imaged under butanol. Image size 1200 nm × 1200 nm. Imaging force ~3–4 nN. *A* indicates entwining of individual polymer strands. *B* corresponds to aggregated regions showing alignment of acetan molecules.

The image shown in Fig. 1 is consistent with the known structural properties of acetan (Morris et al., 1989). The chemical structure of acetan is based on a regular repeat unit (Jansson et al., 1993). This consists of a cellulosic backbone substituted on every second glucose residue with a pentasaccharide side chain (Fig. 2 *A*). X-ray diffraction studies of oriented fibers suggest that acetan adopts a fivefold helical structure of pitch ~4.8 nm (Morris et al., 1989). Optical

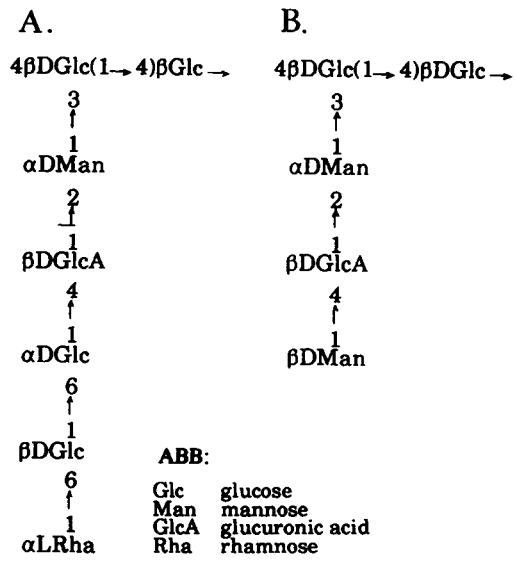

FIGURE 2 Chemical repeat unit structures of (*A*) acetan and (*B*) xanthan omitting base labile noncarbohydrate substituents.

rotation studies on acetan (Morris et al., 1989) are consistent with a thermally reversible order (helix)-disorder (coil) transition within which the helical structure is stabilized at low temperature and high ionic strength. These studies suggest that the helical structure of acetan, observed in the solid state by x-ray diffraction, is retained in aqueous solution. The polysaccharide xanthan has a similar chemical structure (Fig. 2 *B*) (Jansson et al., 1975, 1993; Melton et al., 1976), and both polysaccharides form similar helices (Morris et al., 1989; Millane, 1992). Light scattering studies on xanthan solutions are consistent with Kuhn statistical segment lengths of the order 200 nm and polymer diameters of the order of 2 nm (Coviello et al., 1986).

Within the acetan deposits on the mica, it was noticed that there were regions where the molecules are very concentrated and aligned. Such an aggregated region is marked *B* in Fig. 1. Figs. 3 and 4 show higher resolution images of the acetan within regions such as these. In the semi-ordered regions where the molecular chains have become aligned, the observed chain diameter is much reduced (~2 nm). This effect is consistent with the expected reduction in probe broadening for periodic structures, and the measured diameters are consistent with the values that would be expected for individual acetan helices. In addition, each molecule shows a pronounced variation in contrast along the contour length of the chain. The periodicity of this variation is constant and of the order of 5 nm. Periodic fluctuations in contrast can arise because of electronic noise or inappropriate choice of imaging conditions. The periodicity observed in Figs. 3 and 4, however, is believed to be characteristic of the molecular structure for the following reasons. The period of the contrast variation scales with changes in scan size, although the scanning frequency was kept constant. The contrast variation is observed along the polymer chain irrespective of the orientation of the chain and, furthermore, such contrast fluctuations are not observed on the mica background. Finally, the contrast variation seen in Figs. 3 and 4 has been observed in several subsequent AFM experiments on acetan, each using freshly prepared samples. It is suggested, therefore, that this periodic feature represents the helical structure of the polysaccharide. The large side chain present in acetan may serve to emphasize the variation in thickness along the backbone. The enhanced resolution observed in Figs. 3 and 4 clearly results from the semi-ordered arrangement of the acetan chains within these aggregated regions. This is because the tip does not penetrate between the closely packed molecules to the substrate, and so only the (sharp) apex of the tip interacts with the chains.

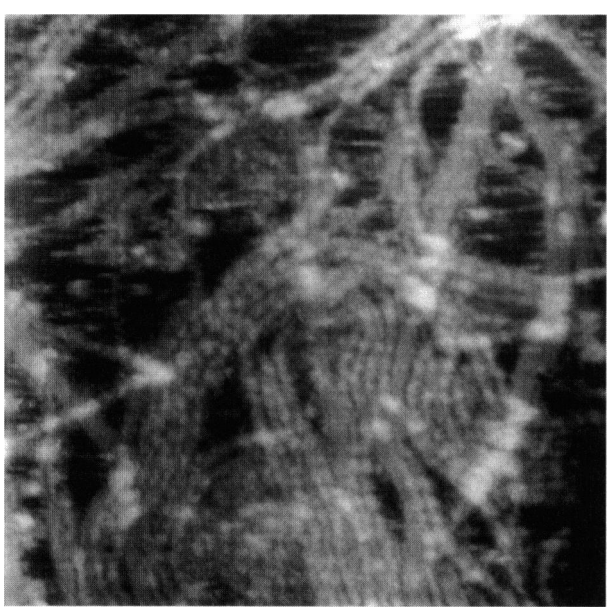

FIGURE 3 High resolution AFM image of aligned polymer strands. Image size 200 nm × 200 nm. Imaging force ~3–4 nN.

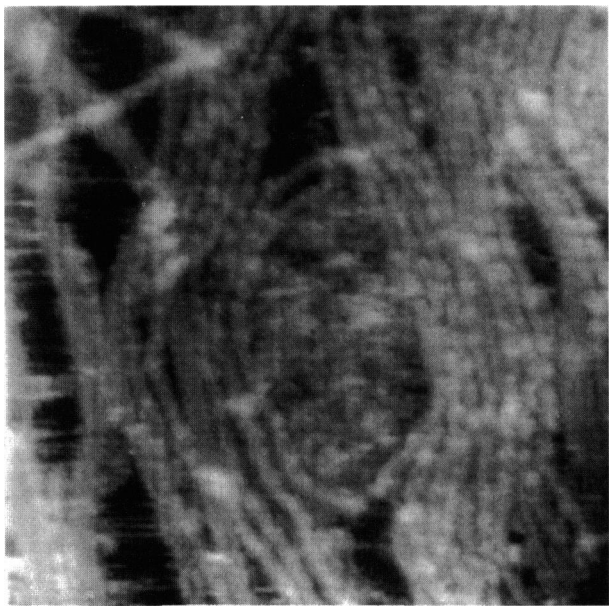

FIGURE 4 High resolution AFM image of aligned acetan molecules. Image size 140 nm × 140 nm. Imaging force ~3–4 nN.

CONCLUSIONS

A simple reproducible method has been developed for imaging uncoated polysaccharide chains by AFM. A crucial aspect of this study was the ability to control the imaging force through the use of butanol. This allowed the fine tuning of image contrast within an appropriate force window. The method has been illustrated through studies on the bacterial polysaccharide acetan. The molecules are revealed as extended stiff coils. Both intra- and inter-molecular entwining has been observed. Measurements of molecular thickness are restricted by probe-broadening effects. Within certain highly concentrated regions of the molecular deposit, the molecules have become aligned. In these semi-ordered 2D arrays, the probe-broadening is reduced and molecular diameters can be estimated. In addition, periodic fluctuations along the polymer chain have been observed and are attributed to the helical structure of the polysaccharide. It remains to be determined whether the present methodology can be applied

generally to image all polysaccharides at such high resolution. The resolution achieved in the present study is substantially higher than that achievable for metal-coated samples using either STM or electron microscopy. Further studies are required to determine whether these methods can be used to investigate complex *irregular* molecular architecture such as polysaccharide branching.

The authors would like to thank Jane Scarll for preparing the figures used in this article.

REFERENCES

Arnott, S. 1977. Ordered conformations of gel forming polysaccharides obtained by x-ray diffraction analysis of oriented fibres. *Dev. Food Carbohydr. Ser. 1.* 43–60.

Bustamante, C., J. Vesenka, C. L. Tang, W. Rees, M. Guthold, and R. Keller. 1992. Circular DNA molecules imaged in air by scanning force microscopy. *Biochemistry.* 31:22–26.

Couso, R. O., L. Ielpi, and M. A. Dankert. 1987. A xanthan-like polysaccharide from *A. xylinum. J. Gen. Microbiol.* 133:2123–2135.

Coviello, T., K. Kajiwara, W. Burchard, M. Dentini, and V. Crescenzi. 1986. Solution properties of xanthan. I. Dynamic and static light scattering from native and modified xanthans in dilute solutions. *Macromolecules.* 19: 2826–2831.

Drake, B., C. B. Prater, A. L. Weisenhorn, S. A. C. Gould, T. R. Albrecht, C. F. Quate, D. S. Cannell, H. G. Hansma, and P. K. Hansma. 1989. Imaging crystals, polymers and processes in water with the AFM. *Science.* 243:1586–1589.

Gunning, A. P., T. J. McMaster, and V. J. Morris. 1993. Scanning tunnelling microscopy of xanthan gum. *Carbohydr. Polym.* 21:47–51.

Hanley, S. J., J. Giasson, J. F. Revol, and D. G. Gray. 1992. Atomic force microscopy of cellulose microfibrils—comparison with TEM. *Polymer.* 33:4639–4642.

Hansma, H. G., M. Bezanilla, F. Zenhausern, M. Adrian, and R. L. Sinsheimer. 1993. Atomic force microscopy of DNA in aqueous solutions. *Nucleic Acids Res.* 21:505–512.

Hansma, H. G., and P. K. Hansma. 1993. Potential applications of atomic force microscopy of DNA to the human genome project. *Proc. SPIE-Int. Soc. Opt. Eng (USA).* 1891:66–70.

Hansma, H. G., C. Sinsheimer, M-Q. Li, and P. K. Hansma. 1992. AFM of single stranded and double stranded DNA. *Nucleic Acids Res.* 20: 3585–3590.

Hansma, H. G., J. Vesenka, C. Siergerist, G. Kelderman, H. Morrett, R. L. Sinsheimer, V. Elings, C. Bustamante, and P. K. Hansma. 1992. Reproducible imaging and dissection of plasmid DNA under liquid with the AFM. *Science.* 256:1180–1184.

Jansson, P.-E., L. Kenne, and B. Lindberg. 1975. Structure of the extracellular polysaccharide from *Xanthomona campestris. Carbohydr. Res.* 45:275–282.

Jansson, P.-E., J. Lindberg, K. M. S. Wimalasiri, and M. A. Dankert. 1993. Structural studies of acetan, an exopolysaccharide elaborated by *Acetobacter xylinum. Carbohydr. Res.* 245:303–310.

Lee, I., E. D. T. Atkins, and M. J. Miles. 1992. Visualisation of the algal polysaccharide carrageenan by scanning tunnelling microscopy. *Ultramicroscopy.* 42–44:1107–1112.

Li, M.-Q., H. G. Hansma, J. Vesenka, G. Kelderman, and P. K. Hansma. 1992. AFM of uncoated plasmid DNA-nanometer resolution with only nanogram amounts of sample. *J. Biomol. Struct. Dyn.* 10: 607–617.

MacCormick, C. A., J. E. Harris, A. P. Gunning, and V. J. Morris. 1993. Characterisation of a variant of the polysaccharide acetan produced by a mutant of *Acetobacter xylinum* strain CR1/4. *J. Appl. Bacteriol.* 74: 196–199.

Melton, L. D., L. Mindt, D. A. Rees, and G. R. Sanderson. 1976. Covalent structure of the extracellular polysaccharide from *Xanthomonas campestris*: evidence from partial hydrolysis studies. *Carbohydr. Res.* 46: 245–257.

Meyer, A., G. Rouquet, J. Lecourtier, and H. Toulhoat. 1992. Characterisation by atomic force microscopy of xanthan in interaction with mica. *In* Physical Chemistry of Colloids and Interfaces in Oil Production. H. Toulhoat and J. Lecourtier, editors. Editions Techniq., Paris, 275–278.

Miles, M. J., I. Lee, and E. D. T. Atkins. 1991. Molecular resolution of polysaccharides by scanning tunnelling microscopy. *J. Vac. Sci. Technol. B.* 9:1206–1209.

Millane, R. P. 1992. Molecular and crystal structures of polysaccharides with cellulosic backbones. *In* Frontiers in Carbohydrate Science 2. R. Chandrasakaran, editor. Elsevier Appl. Sci., London, 168–190.

Morris, V. J., G. J. Brownsey, P. Cairns, G. R. Chilvers, and M. J. Miles. 1989. Molecular origins of acetan solution properties. *Int. J. Biol. Macromol.* 11:326–328.

Murray, M. N., H. G. Hansma, M. Bezanilla, T. Sano, D. F. Ogletree, W. Kolbe, C. L. Smith, C. R. Cantor, S. Spengler, P. K. Hansma, and M. Salmeron. 1993. AFM of biochemically tagged DNA. *Proc. Natl. Acad. Sci. USA.* 90:3811–3814.

Oka, Y., and A. Takahashi. 1992. Scanning tunnelling microscopy of amylose *Kobunshi Ronbunshi.* 49:389–391.

Perez, S., and H. D. Chanzy. 1989. Electron crystallography of linear polysaccharides. *J. Electr. Microsc. Techniques.* 11:280–285.

Perez, S., and J. F. Revol. 1993. Molecular structure and morphology of carbohydrate polymers. *Microsc. Soc. Am. Bull.* 23:28–43.

Rabe, J. P., S. Buchholz, and A. M. Ritcey. 1990. Reactive graphite etch and the structure of an adsorbed organic monolayer-a scanning tunnelling microscopy study. *J. Vac. Sci. Technol. A.* 8:679–683.

Scott, J. E. 1965. Fractionation by precipitation with quaternary ammonium salts. *Methods Carbohydr. Chem.* V:38–44.

Shigekawa, H., T. M. Morozumi, M. Komiyama, M. Yoshimura, A. Kawazu, and Y. Saito. 1991. Scanning tunnelling microscopy on cyclodextrin complexes. *J. Vac. Sci. Technol. B.* 9:1189–1192.

Stokke, B. T., A. Elgsaeter, G. Skjak-Braek, and O. Smidsrød. 1987. The molecular size and shape of xanthan, xylinum, bronchial mucin, alginate, and amylose as revealed by electron microscopy. *Carbohydr. Res.* 160: 13–28.

Thundat, T., D. P. Allison, R. J. Warmack, and T. L. Ferrel. 1992. Imaging isolated strands of DNA molecules by atomic force microscopy. *Ultramicroscopy.* 42–44:1101–1106.

Thundat, T., R. J. Warmack, D. P. Allison, L. A. Bottomley, A. J. Lourenco, and T. L. Ferrel. 1992. Atomic force microscopy of deoxyribonucleic acid strands adsorbed on mica: the effect of humidity on apparent width and image contrast. *J. Vac. Sci. Technol. A.* 10:630–635.

Vesenka, J., M. Guthold, C. L. Tang, D. Keller, E. Delaine, and C. Bustamante. 1992. Substrate preparation for reliable imaging of DNA molecules with the scanning force microscope. *Ultramicroscopy.* 42–44:1243–1249.

Weisenhorn, A. L., P. K. Hansma, T. R. Albrecht, and C. F. Quate. 1989. Forces in AFM in air and water. *Appl. Phys. Lett.* 54:2651–2653.

Wilkins, M. J., M. C. Davies, D. E. Jackson, J. R. Mitchell, C. J. Roberts, B. T. Stokke, and S. J. B. Tendler. 1993. Comparison of scanning tunnelling microscopy and transmission electron microscopy image data of a microbial polysaccharide. *Ultramicroscopy.* 48:197–201.

Yang, X., M. A. Miller, R. Yang, D. F. Evans, and R. D. Edstrom. 1990. Scanning tunnelling microscopic images show a laminated structure for glycogen molecules. *FASEB J.* 4:3140–3143.